Phys. Status Solidi A **210**, No. 12, 2556–2560 (2013) / **DOI** 10.1002/pssa.201329205

physica status solidi a
www.pss-a.com
applications and materials science

Electroluminescence of solution-processed organic light-emitting diodes based on fluorescent small molecules and polymer as hole-transporting layer

Dongdong Wang[1], Zhaoxin Wu*[,2], Xiaoli Lei[3], Wenwen Zhang[3], Bo Jiao[2], Dawei Wang[2], and Xun Hou[2]

[1] School of Science, Department of Applied Chemistry, Xi'an Jiaotong University, No. 28 Xianning West Road, 710049 Xi'an, P.R. China
[2] Key Laboratory for Physical Electronics and Devices of the Ministry of Education, School of Electronic and Information Engineering, Xi'an Jiaotong University, No. 28 Xianning West Road, 710049 Xi'an, P.R. China
[3] School of Science, Xi'an University of Post & Telecommunications, No. 563 Chang'an South Road, 710121 Xi'an, P.R. China

Received 26 March 2013, revised 15 June 2013, accepted 29 July 2013
Published online 4 September 2013

Keywords electroluminescence, optical interference, organic light-emitting diodes, small molecules, solution processing

* Corresponding author: e-mail zhaoxinwu@mail.xjtu.edu.cn, Phone: +860 298 266 4867, Fax: +860 298 266 4867

White organic light-emitting diodes with three successively spin-coated layers, poly(3,4-ethylenedioxythiophene):polystyrene sulfonate, poly(*N*-vinylcarbazole) and small-molecule emissive layer (EML) in turn, and a vacuum-deposited electron-transporting layer (ETL) have been prepared. The EML includes a host bis[2-(4-(*N*,*N*-diphenylamino)phenyl)vinyl] biphenyl, blue dopant 4,4′-bis[2-(4-(*N*,*N*-diphenylamino)phenyl)vinyl]biphenyl (DPAVBi) and yellow dye 5,6,11,12-tetraphenylnaphtacene. The optimized white device shows a current efficiency of 6.7 cd/A (1000 cd/m^2) and a maximum luminance of 16 768 cd/m^2. It was found that the emission spectra of DPAVBi was tuned from blue to greenish blue with increasing of the ETL thickness, which could be attributed to the optical interference effect from the metal cathode. By comparing emission spectra of numerical simulation to tested electroluminescence spectra, the position of the emission zone was determined.

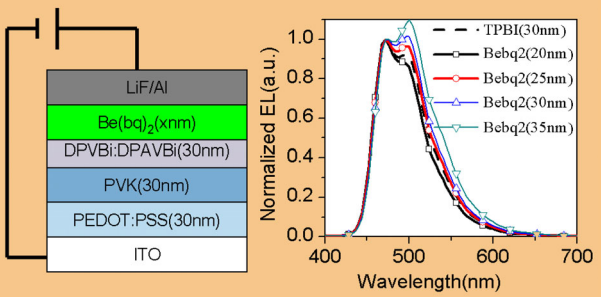

1 Introduction Organic light-emitting devices (OLEDs) have been a subject of intensive research because of their potential applications for flat-panel display and solid-state lighting. Recently, impressive scientific and technological progress has been achieved in this field, and varieties of vacuum-deposited product have been commercialized. Compared to the vacuum-deposited technology, the solution-processed OLEDs are more competitive in flexible and large-sized display applications [1–5] because solution processing are compatible with low-cost, large-area manufacturing process such as screen printing, inkjet printing [6, 7], and it is easy to realize co-doping of multiple dopants and host materials. However, a big challenge of the solution-processed OLEDs is to realize optimized multilayer devices because the solvent of the second layer will dissolve the previous layer. While OLED requires a multilayer device structure to ensure a good performance.

To resolve the above problems, great efforts have been devoted to achieve multilayer device using solution processing. These include using a crosslinking method [8, 9], a liquid buffer layer method [10], a blade-coating method [1], or developing new materials with water/ethanol-soluble polymer [11], and so on. However, these methods for multilayer formation are effective for polymers, but few work well for small-molecule materials, and it is highly

desirable for solution-based fabrication to be applied to small-molecule materials that show excellent efficiency in vacuum-deposited device. For this purpose, several groups have published their results on solution-processed small-molecule devices [12–18]. These devices show comparable performance to those vacuum-deposited counterparts [16, 19]. However, other methods/concepts still need to be developed. In the paper, we begin with a simple fact that most polymers could only dissolve in some specific solvents while organic small molecules could dissolve in most common solvents. Therefore, solution processing should be possible for the multilayer formation when the polymer material is selected as the hole-transporting layer (HTL) and small-molecule material as the light-emitting layer (EML). In the case, the advantages of the polymer materials such as good film-forming nature, and excellent mechanical properties can be wisely combined with high emission efficiency of the small-molecule materials and this is beneficial for realizing efficient OLEDs with cost-effective ways.

Based on the above concept, OLEDs with three successively spin-coating layers and one vacuum-deposited electron-transporting layer (ETL) were fabricated and their performances were investigated. A p-xylene-soluble small-molecule EML was stacked onto a chloroform-soluble PVK (poly(*N*-vinylcarbazole)) HTL, which was formed onto a previously spin-coated PEDOT:PSS layer (poly(3,4-ethylenedioxythiophene): polystyrene sulfonate), to realize solution-processed multilayer OLEDs. A phenomenon that the light emission of the blue dopant was tuned from blue to greenish blue with an increase of the ETL thickness in OLEDs was clearly observed. The effect of wide-angle optical interference by the metal cathode can account for this phenomenon.

2 Experimental A device configuration of indium tin oxide (ITO)/PEDOT:PSS (30 nm)/PVK (30 nm)/EML (30 nm)/ETL (*x* nm)/LiF/Al was used to fabricate solution-processed multilayer OLEDs. Here, the ETL is bis(10-hydroxybenzo[h]qinolinato)beryllium ($Bebq_2$) and the EML is composed of the DPVBi (4,4′-bis(2,2-diphenylvinyl)-1,1′-biphenyl) doped with blue dopant 4,4′-bis[2-(4-(*N*,*N*-diphenylamino)phenyl)vinyl]biphenyl (DPAVBi) and/or 5,6,11,12-tetraphenylnaphtacene (rubrene) for orange emission. The chemical structures of the used materials and detailed device structure, as well as energy levels in the device, are shown in Fig. 1. For device I, the thickness of ETL is fixed at 20 nm and the doping concentration of the DPAVBi in DPVBi varied from 4% to 8%, while for device II, the ETL thickness is changed from 20 to 35 nm with a constant ratio (6%) of DPAVBi:DPVBi. Device III is denoted as a white OLED in which the EML consists of a host DPVBi, doped with 6% DPAVBi for blue emission and 0.6% rubrene for orange emission. The solvent p-xylene was used as an appropriate solvent for dissolving EML materials because it cannot damage the previously applied layer PVK. The details of device fabrication are as follows: The water-dispersed PEDOT:PSS mixture was spin coated on the top of

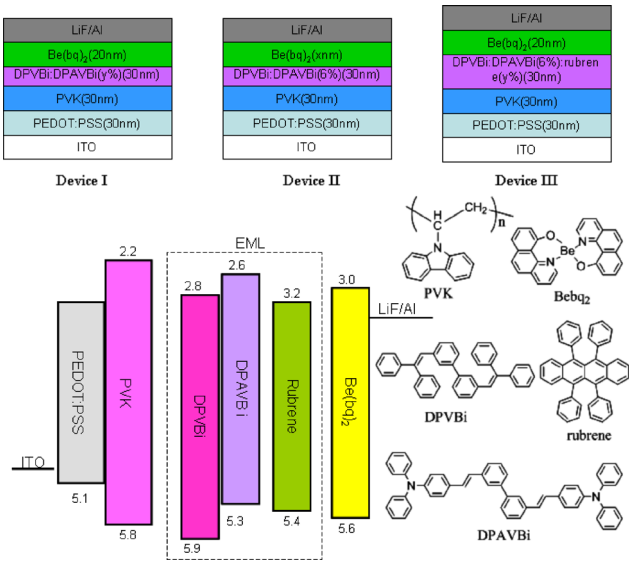

Figure 1 Schematic energy-level diagram of the devices and molecular structures of the used materials.

clean patterned ITO-coated glass substrates in air to achieve a film with a thickness of about 30 nm, which was baked at 139 °C for 30 min, then 30 nm thickness of PVK and EML was deposited by spin coating in turn and baking at 139 °C for 20 and 15 min, respectively. Finally, the samples were loaded into a vacuum chamber for depositing the ETL and cathode, LiF (0.6 nm)/Al (80 nm) by thermal evaporation.

The film thickness was measured by ellipsometers and the EL spectra and CIE coordinates of the devices were measured by a spectrometer (PR650). The current–voltage–luminescence characteristics were analyzed by a Keithley 2602 source meter combining Luminance meter.

3 Results and discussion

3.1 OLEDs performance In our previously published papers [20, 21], it has been demonstrated that the energy-transfer process from DPVBi to DPAVBi can happen efficiently due to the efficient spectra overlap between the blue fluorescent band of DPVBi and the absorption band of DPAVBi. So, the EL characteristics of blue OLEDs were investigated first. Device I (shown in Fig. 1) with various DPAVBi concentrations from 4% to 8% was first fabricated to obtain an optimized doping concentration of DPAVBi. The current efficiency–luminance–current density characteristic curves of device I are shown in Fig. 2a. Among the devices with various doping concentrations of DPAVBi, the device with 6% DPAVBi-doped EML exhibits the best performances, presenting a maximum current efficiency of 4.76 cd/A and a luminance of 13 458 cd/m^2. Furthermore, the doping concentration of DPAVBi was fixed at 6% in EML and the ETL thickness in device II (shown in Fig. 1) varied from 20 to 35 nm and their performance parameters are shown in Fig. 2b. It shows that when the thickness of ETL ($Bebq_2$) changes from 20 to 35 nm the current efficiency of the device slightly increases from 4.76 to 5.41 cd/A.

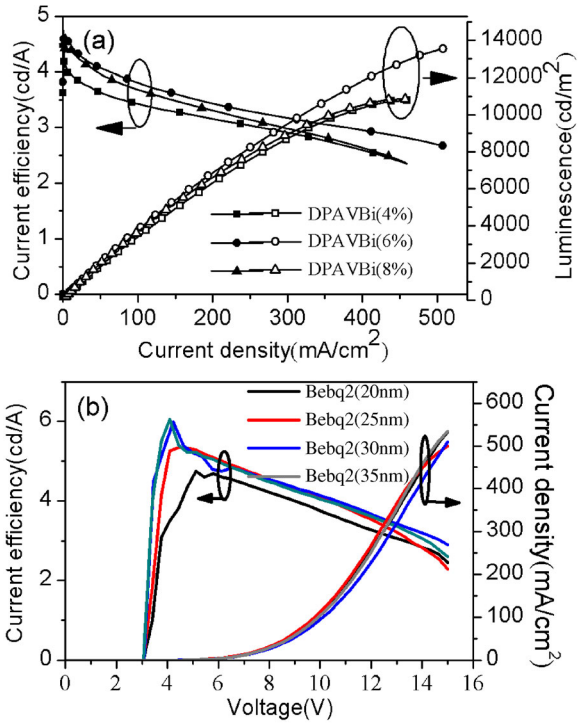

Figure 2 (a) The current efficiency–luminance–current density characteristic curves of device I with various DPAVBi doping concentrations; (b) the current efficiency and density–voltage characteristic curves of device II with various thickness of ETL ($Bebq_2$).

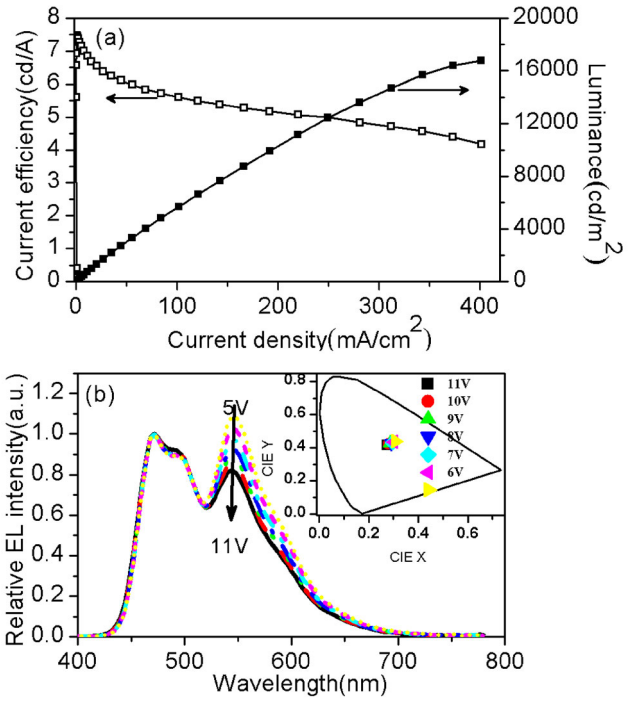

Figure 3 (a) The current efficiency–luminance–current density characteristic curves of device III and (b) its normalized EL spectra under different voltages, the CIE coordinates are in the inset.

Based on the optimized blue OLED, rubrene was further introduced into EML to achieve the white-light emission (device III shown in Fig. 1). When the doping concentration of the rubrene is 0.6%, the two major emission bands at 468 (from DPAVBi) and 552 nm (from rubrene) show nearly equal intensities in normalized EL spectrum (shown in Fig. 3), and a warm white light with a CIE coordinates of (0.308, 0.436) at 1000 cd/m^2 was obtained. It presents a current efficiency of 6.7 cd/A at a luminance of 1000 cd/m^2 and a maximum luminance of 16 768 cd/m^2 (shown in Fig. 3). The efficiency and luminance are better than or comparable to that of the vacuum-deposited or solution-processed white OLEDs in which DPVBi or DPAVBi was used [22–27]. Most of these white OLEDs present a maximum current efficiency ranging from 4.9 cd/A [26] to 14.8 cd/A [27].

3.2 Numerical simulation and discussion It should be particularly noted that the light emission of the blue dopant DPAVBi was significantly tuned from blue to greenish blue with the increase of the ETL ($Bebq_2$) thickness in device II, as shown in Fig. 4a. That is the relative intensity of shoulder peak with 500 nm increases steadily compared to its dominant peak of 468 nm, and it can be seen that when the thickness of the $Bebq_2$ layer increases to 30 and 35 nm, the intensity of the shoulder peak develops into a dominant peak, and as a result, the device emits greenish-blue light. Furthermore, on replacing the 30-nm thickness of $Bebq_2$ layer with the same thickness of TPBi (1,3,5-tri(1-phenyl-1H-benzo[*d*]imidazol-2-yl-phenyl)), the shoulder peak of 500 nm was still clearly observed, indicating the electron-transporting material $Bebq_2$ is not involved in the light-emitting process.

To elucidate the origin of the tuning effect of EL spectra by the $Bebq_2$ thickness, the optical interference effect from the metal cathode was taken into account and numerical simulation of the emission spectra was performed. According to the previous report of Wu et al. [28], the optical schematic of OLEDs was proposed to be simplified as four optical layers, including the metal layer, organic layer consists of PEDOT:PSS, PVK, EML and $Bebq_2$ layer, glass layer, and air layer. Thus, the radiative emission from the exciton was modeled by isotropic oscillating dipoles embedded in the EML and for a sheet of dipoles at a distance z from the cathode reflector, the internal emission intensity can be expressed as follows:

$$I(\theta) \propto |1 + r_s \exp(-2i\delta)|^2 + |1 + r_p \exp(-2i\delta)|^2, \quad (1)$$

$$\delta = 2\pi n z \cos\theta/\lambda + \theta_{s,p},$$

where θ is the emission angle, r_s and r_p are Fresnel reflection coefficient for the s and p polarization, respectively, δ is the

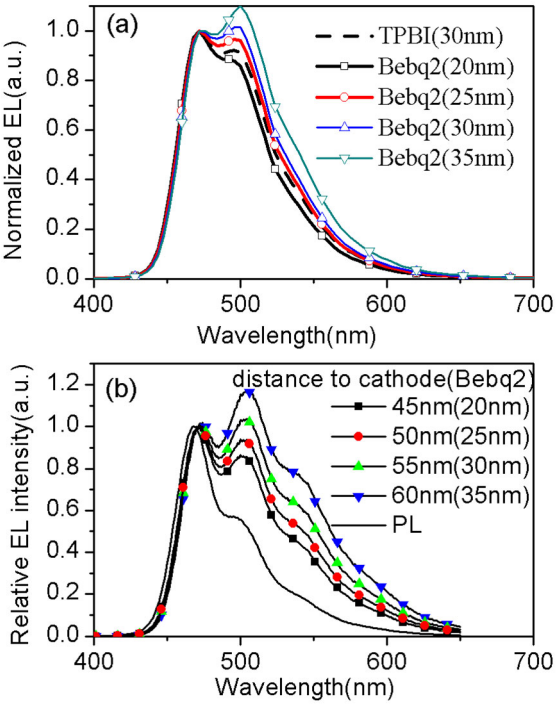

Figure 4 (a) The normalized EL spectra of blue OLEDs with various ETL thickness; (b) the calculated emission spectra of blue OLEDs with various thickness of ETL assuming the emission zone is 5 nm from the interface of PVK/EML (in "b"), the value outside of the bracket is the distance of the emission zone from the cathode and the value in brackets corresponds to the ETL thickness.

phase, and n is the refractive index of the organic materials. Assuming that the position of the emission zone was 5 nm away from the PVK/EML interface, the calculated spectrum of the blue device with various thickness of the $Bebq_2$ layer is shown in Fig. 4b. Here it should be noted that we only considered the wide-angle interference by the cathode and ignored multiple-beam interference effect between the ITO and the metal cathode in our calculation. Interestingly, the calculated emission spectra are well in accord with the experimental results. For the $Bebq_2$ layer, with the thickness of 20 and 25 nm, the peak around 468 nm in the calculated spectrum dominates, and while with the thickness of 30 and 35 nm, the shoulder peak around 500 nm becomes dominant in the whole spectrum. By the comparison of the numerical results and EL spectra of the blue OLEDs, the emission zone of the present device is determined to be located at the PVK/EML interface. It is reasonable because $Bebq_2$, which exhibits an electron mobility of about one order of magnitude higher than that of tris-(8-hydroxyquinoline) aluminum (Alq_3) [29], is an efficient electron-transporting material and the DPVBi is a material with bipolar-transporting property [30]. As a result, the variable thickness of the $Bebq_2$ layer has little effect on the location of the emission zone. This can be supported from their characteristic curves of current density–voltage (see Fig. 1b) that shows nearly complete superposition.

4 Conclusions In conclusion, based on the solubility difference between the polymer and the small molecule we presented a concept of forming a multilayer device. The concept wisely combined polymers as hole-injecting/transporting layer and small-molecule materials as EML with little restriction on solvents. We also found that the EL spectra of the DPAVBi in device II significantly depended on the thickness of the ETL, which can be attributed to the effect of wide-angle optical interference by the metal cathode.

Acknowledgements This work has been supported by the Fundamental Research Funds for the Central Universities (Grant No. 08143034), the Basic Research Program of China (2013CB328705), National Natural Science Foundation of China (Grant Nos. 61275034 and 61106123).

References

[1] S.-R. Tseng, H.-F. Meng, K.-C. Lee, and S.-F. Horng, Appl. Phys. Lett. **93**, 153308 (2008).
[2] J. N. Yao and Y. S. Zhao, Adv. Mater. **25**, 3627 (2013).
[3] C. D. Muller, A. Falcou, N. Reckefuss, M. Rojahn, V. Wiederhirn, P. Rudati, H. Frohne, O. Nuyken, H. Becker, and K. Meerholz, Nature **421**, 829 (2003).
[4] Z. Ge, T. Hayakawa, S. Ando, M. Ueda, T. Akiike, H. Miyamoto, T. Kajita, and M.-A. Kakimoto, Adv. Funct. Mater. **18**, 584 (2008).
[5] B. C. Krummacher, V. E. Choong, M. K. Mathai, S. A. Choulis, F. So, F. Jermann, T. Fiedler, and M. Zachau, Appl. Phys. Lett. **88**, 113506 (2006).
[6] M. Singh, H. M. Haverinen, P. Dhagat, and G. E. Jabbour, Adv. Mater. **22**, 673 (2010).
[7] H. Gorter, M. J. J. Coenen, M. W. L. Slaats, M. Ren, W. Lu, C. J. Kuijpers, and W. A. Groen, Thin Solid Films **532**, 11 (2013).
[8] J. Li, T. Sano, Y. Hirayama, T. Tomita, H. Fujii, and K. Wakisaka, J. Appl. Phys. **100**, 034506 (2006).
[9] C. A. Zuniga, J. Abdallah, W. Haske, Y. Zhang, I. Coropceanu, S. Barlow, B. Kippelen, and S. R. Marder, Adv. Mater. **25**, 1739 (2013).
[10] S. R. Tseng, S. C. Lin, H. F. Meng, H. H. Liao, C. H. Ye, H. C. Lai, S. F. Horng, and C. S. Hsu, Appl. Phys. Lett. **88**, 163501 (2006).
[11] S. Wang, D. Moses, G. Bazan, A. J. Heeger, and X. Gong, Adv. Mater. **17**, 2053 (2005).
[12] Z. Ge, T. Hayakawa, S. Ando, M. Ueda, T. Akiike, H. Miyarnoto, T. Kajita, and M.-A. Kakimoto, Chem. Mater. **20**, 2532 (2008).
[13] S. Feng, L. Duan, L. D. Hou, J. Qiao, D. Q. Zhang, G. F. Dong, L. D. Wang, and Y. Qiu, J. Phys. Chem. C **115**, 14278 (2011).
[14] L. A. Duan, L. D. Hou, T. W. Lee, J. A. Qiao, D. Q. Zhang, G. F. Dong, L. D. Wang, and Y. Qiu, J. Mater. Chem. **20**, 6392 (2010).
[15] J. H. Jou, M. C. Sun, H. H. Chou, and C. H. Li, Appl. Phys. Lett. **87**, 043508 (2005).
[16] N. Rehmann, D. Hertel, K. Meerholz, H. Becker, and S. Heun, Appl. Phys. Lett. **91**, 243512 (2007).
[17] J. D. You, S. R. Tseng, H. F. Meng, F. W. Yen, I. F. Lin, and S. F. Horng, Org. Electron. **10**, 1610 (2009).

[18] A. Kohnen, M. Irion, M. C. Gather, N. Rehmann, P. Zacharias, and K. Meerholz, J. Mater. Chem. **20**, 3301 (2010).
[19] M. K. Mathai, V. E. Choong, S. A. Choulis, B. Krummacher, and F. So, Appl. Phys. Lett. **88**, 103507 (2006).
[20] D. Wang, Z. Wu, X. Zhang, B. Jiao, S. Liang, D. Wang, R. He, and X. Hou, Org. Electron. **11**, 641 (2010).
[21] D. Wang, Z. Wu, X. Zhang, D. Wang, and X. Hou, J. Lumin. **130**, 321 (2010).
[22] W. Song, M. Meng, Y. H. Kim, C.-B. Moon, C. G. Jhun, S. Y. Lee, R. Wood, and W.-Y. Kim, J. Lumin. **132**, 2122 (2012).
[23] J. Wang, Y. Zhao, W.-F. Xie, Y. Duan, P. Chen, and S.-Y. Liu, Acta Phys. Sin. **60**, 107203 (2011).
[24] H.-P. Lin, F. Zhou, J. Li, X.-W. Zhang, L. Zhang, X.-Y. Jiang, Z.-L. Zhang, and J.-H. Zhang, Phys. Status Solidi A **209**, 401 (2012).
[25] Q. Xue, G. Xie, P. Chen, J. Lu, D. Zhang, Y. Tang, Y. Zhao, J. Hou, and S. Liu, Synth. Met. **160**, 829 (2010).
[26] H. Huang, Q. Fu, S. Zhuang, G. Mu, L. Wang, J. Chen, D. Ma, and C. Yang, Org. Electron. **12**, 1716 (2011).
[27] S. Ye, J. Chen, C.-A. Di, Y. Liu, K. Lu, W. Wu, C. Du, Y. Liu, Z. Shuai, and G. Yu, J. Mater. Chem. **20**, 3186 (2010).
[28] Z. Wu, L. Wang, G. Lei, and Y. Qiu, J. Appl. Phys. **97**, 103105 (2005).
[29] J. H. Lee, C. I. Wu, S. W. Liu, C. A. Huang, and Y. Chang, Appl. Phys. Lett. **86**, 103506 (2005).
[30] E. I. Haskal, Synth. Met. **91**, 187 (1997).

